

Momentum state engineering and control in Bose-Einstein condensates

Sierk Pötting^{1,2,3*}, Marcus Cramer^{1,4}, and Pierre Meystre¹

¹*Optical Sciences Center, University of Arizona, Tucson, Arizona 85721*

²*Max-Planck-Institut für Quantenoptik, 85748 Garching, Germany*

³*Sektion Physik, Universität München, 80333 München, Germany*

⁴*Fachbereich Physik der Philipps-Universität, 35032 Marburg, Germany*

(June 8, 2024)

We demonstrate theoretically the use of genetic learning algorithms to coherently control the dynamics of a Bose-Einstein condensate. We consider specifically the situation of a condensate in an optical lattice formed by two counter-propagating laser beams. The frequency detuning between the lasers acts as a control parameter that can be used to precisely manipulate the condensate even in the presence of a significant mean-field energy. We illustrate this procedure in the coherent acceleration of a condensate and in the preparation of a superposition of prescribed relative phase.

PACS numbers: 03.75.Fi, 32.80.Qk

I. INTRODUCTION

Atomic Bose-Einstein condensates (BEC) are now generated almost routinely in the laboratory, and are resulting in numerous applications in fundamental and applied science. A key element of this research is the ability to coherently engineer and control the state of the condensate and its dynamics. This is for example the case in the generation of atomic solitons [1–3], which requires that a precise phase be imprinted on the condensate; atomic four-wave mixing, which involves the splitting of a condensate into three momentum groups [4]; the mixing of optical and matter waves [5–9], which again requires the splitting of a condensate; mode-locked atom lasers [10], where a condensate wave function is spatially modulated by a periodic optical potential, etc. It can be expected that the preparation of condensate states of increasing sophistication will be required in future applications, including atom lithography [11,12] and atom holography [13].

The coherent manipulation and control of quantum states has been the subject of considerable work in many other areas of physics. For example, it is now possible to precisely carve the electronic wave function of atoms or to excite vibrational modes of molecules [14–16], using precisely engineered optical pulses. Similar techniques have lead to spectacular advances in nonlinear optics.

A common tool to many of these developments is the use of genetic algorithms. These multi-dimensional opti-

mization techniques proceed by parametrizing a control function in terms of a finite set of coefficients, or “genes”, a particular set of genes being called a “chromosome.” The genetic algorithm operates on a set of chromosomes, the “population.” Its success in achieving a design goal is quantified by a “fitness function,” a measure of how close the action of a particular chromosome is to the desired state. The algorithm proceeds by replacing an ill-fitted fraction of the population by new chromosomes, the “offsprings”, that result from the mating of two parent chromosomes according to some set of rules; see e.g. Refs. [17,18] for details. In addition to that controlled combination of chromosomes, random mutations on single genes prevent the algorithm from getting trapped in local extrema. The process is iterated until one chromosome reaches a prescribed fitness value.

Because of collisions, the dynamics of atomic BEC is intrinsically nonlinear. Hence, it is difficult in general to precisely predict the effects of control fields on the condensate properties. Indeed, condensates are emerging as excellent test systems to study quantum chaos [19,20]. This is a clear indication that straightforward analytical tools are generally unlikely to be sufficient in the coherent manipulation and control of BEC. It is therefore natural to turn instead to the use of genetic algorithms. The main goal of this paper is to illustrate how they can be applied to the design of specific momentum states of condensates.

We specifically consider two examples, the acceleration of a condensate, and the preparation of a BEC in a coherent superposition of two momentum states with a prescribed phase difference. The external control is provided by two counterpropagating laser fields of adjustable frequency that provide a time-dependent optical lattice interacting with the condensate via Bragg scattering. This is a natural choice, since Bragg scattering is a well-established tool of atom optics: It has been used in many applications such as the determination of the coherence properties of condensates [21,22], the implementation of Mach-Zehnder interferometers to image the condensate phase [23], the splitting of condensates [24], and the creation of initial states appropriate for nonlinear mixing processes [4]. Optical lattices have also been used to investigate physical effects such as atomic Landau-Zener tunneling [25,26], Bloch oscillations [27–29], and the acceleration of BECs [30]. Recently, a Josephson junction array was experimentally realized with a BEC

*email: sierk.poetting@optics.arizona.edu

in an optical standing wave [31].

The paper is organized as follows: Section II discusses the model, establishes our notation, and introduces the “quasi-modes” of the condensate used in the subsequent analysis. Section III briefly reviews important aspects of genetic algorithms. The main results are presented in section IV, which illustrates the usefulness of genetic algorithms in condensate acceleration and in the preparation of macroscopically separated momentum states of prescribed relative phase. Finally, section V is a summary and conclusion. Appendix A gives further details of the genetic algorithm.

II. MODEL

We consider a condensate consisting of N atoms of mass M at temperature $T = 0$, and placed in a frequency-chirped optical lattice formed by two counterpropagating laser beams of wave vector k_L and central frequency ω_0 . The electric field is then given by

$$E(z, t) = \frac{\mathcal{E}_0}{2} \left[e^{i(k_L z - (\omega_0 + \delta(t))t)} + e^{-i(k_L z + \omega_0 t)} + c.c. \right], \quad (1)$$

where $\delta(t)$ is a time-dependent frequency difference between the two beams. We define the detuning Δ from the atomic resonance as $\Delta = \omega_a - \omega_0$, with ω_a being the atomic transition frequency. In order to avoid spontaneous emission we use far-off resonance light, so that $|\Delta| \gg \Gamma$, with Γ the spontaneous decay rate of the excited atomic level. We assume that the coupling of the light field from Eq. (1) to the atomic system is characterized by a Rabi frequency $\Omega = d\mathcal{E}_0/\hbar$, where d is the dipole matrix element of the transition. If the Rabi frequency is small compared to the detuning, $|\Omega| \ll |\Delta|$, we can adiabatically eliminate the excited atomic level, which evolves on a much faster time scale than the lower level. Making use of the rotating wave approximation which neglects terms varying at twice the optical frequency ω_0 , the resulting time-dependent optical potential for the lower atomic level is then given by

$$V(z, t) = V_0 \cos[2k_L z - \delta(t)t], \quad (2)$$

where $V_0 = \hbar|\Omega|^2/2\Delta$ is the lattice depth (see also Ref. [32] for details). In order not to violate the adiabatic approximation, the detuning $\delta(t)$ must remain small compared to the detuning Δ , and vary slow on the fast time scale:

$$|\delta| \ll |\Delta|, \quad \left| \frac{d\delta}{dt} \right| \ll \Delta^2. \quad (3)$$

The instantaneous phase velocity of the lattice fringes in Eq. (2),

$$v_{\text{lat}}(t) \approx \left(\frac{1}{2k_L} \right) \frac{\partial[\delta(t)t]}{\partial t}, \quad (4)$$

must remain much smaller than the speed of light at all times in order to neglect any time-dependence of the wavenumber k_L , as discussed in detail in Ref. [33].

The control of the state of the BEC is achieved by imposing a time dependence on the detuning $\delta(t)$ between the counterpropagating laser beams. It is this time dependence that is to be determined by the genetic algorithm.

We assume that the condensate is tightly confined in the transverse direction, so that the system can be described semiclassically by a one-dimensional time-dependent Gross-Pitaevskii equation (GPE). The condensate evolution in the optical lattice of Eq. (2) is then given by

$$i\hbar \frac{\partial}{\partial t} \psi(z, t) = \left[-\frac{\hbar^2}{2M} \frac{\partial^2}{\partial z^2} + V(z, t) \right] \psi(z, t) + NU_0 |\psi(z, t)|^2 \psi(z, t), \quad (5)$$

where $\psi(z, t)$ is the condensate wave function, $U_0 = 4\pi\hbar^2 a/M$, and a , the s -wave scattering length reduced to one dimension, is taken to be positive. In the presence of a periodic potential, one needs to be aware of the possible fragmentation of the condensate via a Mott insulator transition. Ref. [34] investigates this problem, predicting the onset of fragmentation when the lattice potential depths are in excess of 5-10 lattice recoil energies. Here we consider only situations where the lattice potential is shallow enough that such fragmentation does not occur. Superfluid effects can likewise be ignored, since the critical velocity for typical Bose-Einstein condensates was recently experimentally determined to lie in the mm/s regime [35-37] and as we show shortly, Bragg diffraction only populates momentum side modes of the condensate, spaced by momenta $2\hbar k_L$, corresponding to velocities far exceeding the critical velocity.

Our goal in this paper is to manipulate the momentum of the condensate. It is therefore convenient to introduce the momentum space condensate wave function

$$\phi(k, t) = \frac{1}{\sqrt{2\pi}} \int_{-\infty}^{\infty} dz \psi(z, t) e^{-ikz}. \quad (6)$$

Substituting these into Eq. (5) we obtain the corresponding coupled difference-differential GPEs

$$i\hbar \frac{\partial}{\partial t} \phi(k, t) = \frac{\hbar^2 k^2}{2M} \phi(k, t) + \frac{V_0}{2} \left[\phi(k - 2k_L) e^{-i\delta(t)t} + \phi(k + 2k_L) e^{i\delta(t)t} \right] + \frac{NU_0}{2\pi} \int dk_1 dk_2 \phi(k - k_1 + k_2, t) \phi(k_1, t) \phi^*(k_2, t). \quad (7)$$

The spatial extent of the condensates that we have in mind is large compared to the lattice period π/k_L . Their initial momentum distribution is therefore much narrower than k_L , $\Delta k \ll k_L$. From Eq. (7), we observe

that the optical lattice couples states separated in momentum by $k = \pm 2k_L$, and hence leads to a momentum distribution consisting in general of a “comb” of narrow peaks of width Δk . Ground state collisions lead to a broadening of these peaks, but for small enough particle numbers N , it can be expected that this broadening remains small compared to $2k_L$. This suggests that it is useful to expand the momentum space condensate wave function on a basis of “quasi-modes” described by the orthonormal mode functions

$$u_n(k) = \frac{1}{2k_L} \{ \Theta[(2n-1)k_L] - \Theta[(2n+1)k_L] \} \quad (8)$$

as

$$\phi(k, t) = \sum_n \zeta_n(t) u_n(k), \quad (9)$$

where

$$\zeta_n(t) = \int_{-\infty}^{\infty} dk u_n(k) \phi(k, t) = \int_{(2n-1)k_L}^{(2n+1)k_L} dk \phi(k, t) \quad (10)$$

and the step function $\Theta(x)$ is defined as

$$\Theta(x) = \begin{cases} 0 & : x < 0 \\ 1 & : x \geq 0 \end{cases} \quad (11)$$

The associated “quasi-mode” populations $p_n(t)$ are accordingly

$$p_n(t) = |\zeta_n(t)|^2 = \int_{(2n-1)k_L}^{(2n+1)k_L} dk |\phi(k, t)|^2. \quad (12)$$

In the following, we use a genetic algorithm to find a time-dependent detuning $\delta(t)$ leading to predetermined values of the probability amplitudes $\zeta_n(t)$. Before presenting selected results of this study, though, we review for completeness some important aspects of this optimization technique.

III. GENETIC ALGORITHM

Genetic algorithms proceed by parametrizing a control function in terms of a finite set of genes, a particular set of genes being called a chromosome. The genetic algorithm operates on a set of chromosomes, the population, whose action on the system to be controlled is quantified in terms of a fitness function. In the situation at hand, the control is achieved by the time-dependent detuning $\delta(t)$, expressed by a truncated Fourier series

$$\delta_i(t) = \sum_{\nu=1}^m a_{i\nu} \cos(\nu\omega_R t) + b_{i\nu} \sin(\nu\omega_R t), \quad i = 1, \dots, \mathcal{N}, \quad (13)$$

where $\omega_R = \hbar k_L^2/M$ is the recoil frequency. Each detuning δ_i is encoded in a chromosome c_i consisting of

$n = 2m$ genes g_{ij} , each gene corresponding to one particular Fourier coefficient,

$$c_i(g_{i1}, \dots, g_{in}) = c_i(a_{i1}, \dots, a_{im}, b_{i1}, \dots, b_{im}). \quad (14)$$

The index i labels a specific chromosome, and the size of the chromosome population is \mathcal{N} .

Starting from a randomly initialized population, the genetic algorithm uses a set of mating rules, mutations, and a problem-specific fitness function $f(c_i)$ to create new generations of chromosomes, as illustrated in Fig.1.

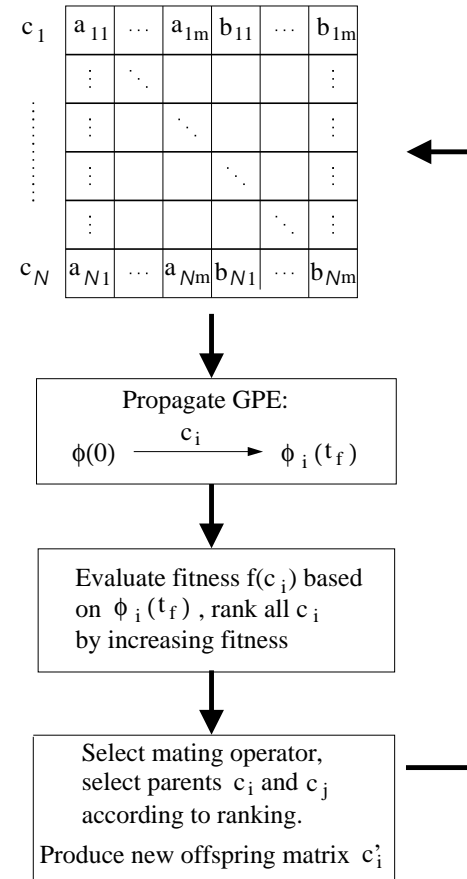


FIG. 1. Schematics of the genetic algorithm: In our problem, the fitness is evaluated by evolving an initial momentum space wavefunction $\phi(0)$ according to the GPE from Eq. (5) for a time t_f , the dynamics of the optical lattice being determined by the detuning $\delta_i(t)$. The final wavefunction is then compared to the optimization goal.

The first step consists in selecting parent chromosomes that are to be combined by mating operators. This is achieved by ranking the initial \mathcal{N} chromosomes according to their fitness and using the so-called “roulette wheel” method [17] to preferentially select parent chromosomes with a high fitness.

In the next step mating operators are selected that generate a group of “offspring” chromosomes c'_i from the “parent” population c_i . As such, these operators are at the heart of the genetic algorithm.

Several mating operators may be considered: The “one-point-crossover” operator cuts the two parent chromosomes at a randomly chosen position μ and swaps the genes according to

$$\begin{aligned}
&c_1(g_{11}, \dots, g_{1n}) \\
&c_2(g_{21}, \dots, g_{2n}) \\
&\downarrow \\
&\text{1-point-crossover} \tag{15} \\
&\downarrow \\
&c'_1(g_{11}, \dots, g_{1\mu}, g_{2,\mu+1}, \dots, g_{2n}) \\
&c'_2(g_{21}, \dots, g_{2\mu}, g_{1,\mu+1}, \dots, g_{1n}),
\end{aligned}$$

with $1 \leq \mu \leq n$. A slightly modified version of this operator is the “two-point-crossover” operator that cuts the two parent chromosomes at two random positions μ_1 and μ_2 and then exchanges the genes between these two positions:

$$\begin{aligned}
&c_1(g_{11}, \dots, g_{1n}) \\
&c_2(g_{21}, \dots, g_{2n}) \\
&\downarrow \\
&\text{2-point-crossover} \tag{16} \\
&\downarrow \\
&c'_1(g_{11}, \dots, g_{1\mu_1}, g_{2,\mu_1+1}, \dots, g_{2,\mu_2-1}, g_{1\mu_2}, \dots, g_{1n}) \\
&c'_2(g_{21}, \dots, g_{2\mu_1}, g_{1,\mu_1+1}, \dots, g_{1,\mu_2-1}, g_{2\mu_2}, \dots, g_{2n}),
\end{aligned}$$

with $1 \leq \mu_1 \leq \mu_2 \leq n$.

Another type of mating operator, the “average-crossover” operator, produces just one offspring from the two parent chromosomes by averaging the genes between two randomly chosen positions μ_1 and μ_2 :

$$\begin{aligned}
&c_1(g_{11}, \dots, g_{1n}) \\
&c_2(g_{21}, \dots, g_{2n}) \\
&\downarrow \\
&\text{average-crossover} \tag{17} \\
&\downarrow \\
&c'_1(g_{11}, \dots, g_{1\mu_1}, g'_{\mu_1+1}, \dots, g'_{\mu_2-1}, g_{1\mu_2}, \dots, g_{1n}),
\end{aligned}$$

with $1 \leq \mu_1 \leq \mu_2 \leq n$ and $g'_\kappa = (g_{1\kappa} + g_{2\kappa})/2$.

Except for the random location at which the splicing of the chromosome occurs, the mating algorithms discussed so far are deterministic. In addition, genetic algorithms also require the use of “mutation” and “creep.” These are random operators that produce one offspring from one parent by altering any gene of the parent chromosome with a given probability called the mutation rate, respectively the creep rate:

$$\begin{aligned}
&c(g_1, \dots, g_n) \\
&\downarrow \\
&\text{mutation, creep} \tag{18} \\
&\downarrow \\
&c'(g_1, \dots, g'_\mu, \dots, g_n).
\end{aligned}$$

The mutation operator chooses g'_μ randomly within some bounds, whereas the creep operator shifts the old value g_μ by a random amount, $g'_\mu = g_\mu + (0.5 - r)p_{\text{creep}}$. Here p_{creep} is a parameter that controls the range of the shift and $0 \leq r \leq 1$ a random number.

The operators discussed in this section are the only ones used in our analysis. When it comes to selecting a specific mating operator, there are basically two possibilities: The first one consists of assigning fixed weights to the available operators and then choosing randomly among them. This is a straightforward approach, but it suffers from the problem of not discriminating against mating operators that do not perform well for the optimization problem at hand. Thus, a second possibility is to dynamically adjust the operator weights over the course of the optimization [17,38]. This guarantees that the best suited operators are applied and allows one to test the performance of new mating operators. This is done by assigning an adjustable “operator fitness” to each mating operator under consideration. As such, the mating operators are selected according to their fitness the same way as the parent chromosomes are picked. The details of the procedure used in our simulations are discussed in the next section and also in the appendix.

IV. RESULTS

A. Coherent acceleration

We now apply the genetic algorithm approach to the manipulation of the state of a BEC in a chirped optical lattice. As a first example, we consider the coherent transfer of a condensate population between the adjacent quasi-modes u_0 and u_1 . Our motivation here is the need to find efficient ways to accelerate condensates for atom optics applications. This problem was theoretically analyzed in Refs. [39,33] and experimentally demonstrated in Ref. [30] for the case of a linear dependence of $\delta(t)$, $\delta(t) = \eta t$. While this chirping of the lattice detuning does lead to a large mean acceleration of the condensate, it unfortunately leaves a substantial fraction of the condensate in lower quasi-modes. This translates into a loss in coherence that is unacceptable, e.g., in interferometric applications. The question, then, is whether an optimized time-dependent detuning determined by a genetic algorithm can eliminate this problem.

For the sake of illustration, we assume that the condensate is initially in the zero-momentum quasi-mode, $p_0(t=0) = 1$, and seek a time-dependent detuning such that $p_1(t_f) = 1$ after some predetermined time t_f . In that case, the algorithm fitness has the simple form

$$f(c_i) = p_1(t_f), \tag{19}$$

with an optimal value of unity.

Fig. 2 summarizes the results of the optimization procedure. It compares the optimized population transfer

of a fairly large condensate consisting of 10^6 atoms to the case of the same condensate subject to on-resonance Bragg scattering. In this example, the genetic algorithm involved a one-point-crossover, a two-point-crossover and an average cross-over mating operator. In addition, it included two mutation operators with mutation rates of 0.8 and 0.4, and two creep operators, both at a rate of 0.9, but different creep parameters, a “coarse” creep with $p_{\text{creep}} = 0.01$ and a “finer” creep operator with $p_{\text{creep}} = 0.001$. More details of the simulations are given in the appendix.

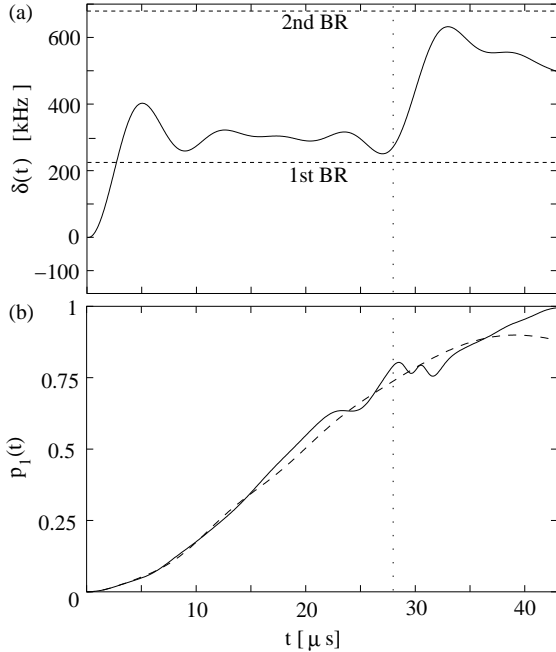


FIG. 2. Momentum transfer of a Sodium condensate with a Gaussian spatial distribution of longitudinal width $50 \mu\text{m}$ and transverse width $5 \mu\text{m}$; $\lambda_L = 985 \text{ nm}$ and $V_0 = \hbar\omega_R$, $M = 3.82 \cdot 10^{-26} \text{ kg}$ and $a_s = 4.9 \text{ nm}$. (a) The solid line is the optimized time-dependent detuning. The dotted lines label the first and second Bragg resonance (BR) for reference. (b) Temporal evolution of the mode population p_1 for $N = 2 \cdot 10^6$ atoms: On resonance (dashed) and optimized (solid). The vertical dotted line denotes the time it takes to resonantly transfer all population to the quasi-mode u_1 in a linear two-mode system.

While it can be expected that resonant Bragg scattering at the appropriate frequency transfers perfectly the population of a small condensate from mode u_0 to mode u_1 , such is not the case for the large condensate we investigated (dashed line in Fig. 2). In this case, the mean-field nonlinearity of the condensate is no longer negligible. It dynamically shifts the Bragg resonance [40] so that the transfer efficiency drops to barely over 90% and the maximum transfer occurs later in time. It is in such nontrivial situations that genetic algorithms are expected to be useful. Indeed, the optimal time-dependent detuning $\delta(t)$

found by the genetic algorithm is highly non-trivial. The temporal dependence of the detuning $\delta(t)$, which transfers more than 99% of the population to the quasi-mode u_1 , reveals that while it is initially advantageous to remain close to the Bragg resonance frequency, as indicated by the rather flat portion of the detuning, it eventually becomes necessary to drastically couple the condensate atoms to higher momentum modes so as to drag the remaining population to the final state u_1 [41].

The effect of the mean-field energy is further illustrated in Fig. 3, which shows the final momentum distribution $\phi_1(k)$ within the quasi-mode u_1 for various numbers of atoms in the condensate for optimal transfer. While this distribution remains extremely narrow compared to the quasi-mode width $2k_L$, collisions lead to a substantial reshaping and broadening within that mode.

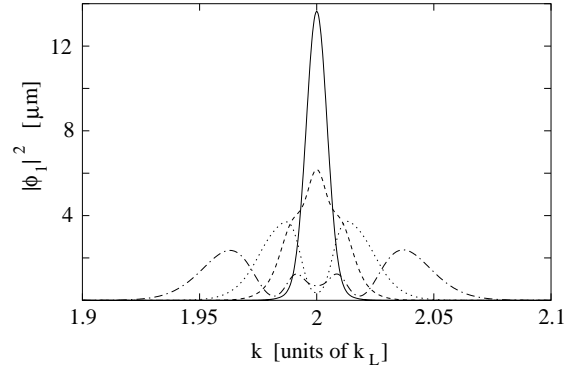


FIG. 3. Effect of the nonlinearity on the momentum space wave function: Momentum space densities within quasimode u_1 after optimizing the transfer, so that $p_1 > 0.99$ after time $t_f = 43 \mu\text{s}$; $N = 1 \cdot 10^5$ (solid), $N = 5 \cdot 10^5$ (dashed), $N = 1 \cdot 10^6$ atoms (dotted), and $N = 2 \cdot 10^6$ (dashed-dotted).

B. Coherent superposition

In a second application, we set out to design an equal-weight superposition of the two quasi-mode states u_0 and u_1

$$\phi(k, t_f) = \frac{1}{\sqrt{2}} (u_0 e^{i\varphi_0} + u_1 e^{i\varphi_1}), \quad (20)$$

with a prescribed relative phase $\Delta\varphi = \varphi_1 - \varphi_0$. In contrast to the previous example, we now want to control two properties of the quantum state, the relative phase as well as the population in each state. The fitness function to be optimized is therefore more complicated.

We choose to employ a so-called “penalty function” $P(c_i)$ for the optimization of the quasi-mode populations [18]. The goal of $P(c_i)$ is to decrease the fitness of chromosomes that do not fulfill the desired requirements, thereby steering the population towards the target values. A prototype penalty function is

$$P(c_i) = \begin{cases} 1.5 & : p_0(c_i), p_1(c_i) > 0.465 \\ 1.0 & : p_0(c_i), p_1(c_i) > 0.47 \\ 0 & : p_0(c_i), p_1(c_i) > 0.475 \\ 100 & : \text{else} \end{cases} \quad (21)$$

The fitness function for this optimization problem is then given by

$$f(c_i) = 1 - |\alpha(c_i) - \Delta\varphi| - P(c_i), \quad (22)$$

where, as we recall, c_i corresponds to a specific realization of the time-dependent detuning $\delta(t)$ and $\alpha(c_i)$ is the relative phase corresponding to this realization. This fitness function reaches its maximum, unity in this case, when the populations are within the specified range and the phase difference is exactly as prescribed. The results for the optimization for the two cases $\Delta\varphi = -\pi/2$ and $\Delta\varphi = -\pi/4$ are shown in Fig. 4. For the genetic algorithm we used the same operators and their parameters as in Sec. IV A. More details of the simulations are given in the appendix.

Fig. 5 shows the momentum distributions $\phi_0(k)$ and $\phi_1(k)$ of the condensate within each of the two quasi-modes u_0 and u_1 , as well as the corresponding phases for the case $\Delta\varphi = -\pi/2$. Clearly, the genetic algorithm converges to the stated goal, and produces a condensate in the desired coherent superposition.

In particular, we observe that the relative phase of the two components is approximately constant in the region where the condensate wave function is different from zero. The optimization goal of $\Delta\varphi = -\pi/2$ is achieved with an accuracy of over 99% at the center of the mode. The curvature of the phase at the wings of the wave function is due to nonlinear phase shifts accumulated during the Hamiltonian evolution. It could be reduced by decreasing the number of atoms in the condensate.

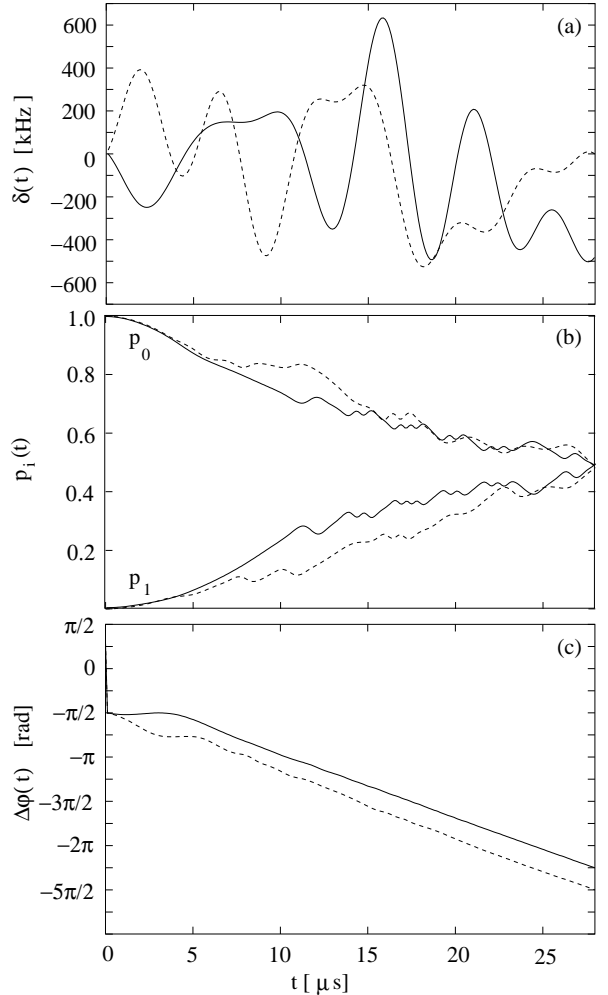


FIG. 4. Excitation of an equal-weight coherent superposition of momentum states with relative phases, $\Delta\varphi = -\pi/4$ (solid) and $\Delta\varphi = -\pi/2$ (dashed). The parameters are the same as in Fig. 2, except that the condensate has a Gaussian spatial distribution of longitudinal width $100 \mu\text{m}$ and $N = 5 \cdot 10^4$. (a) Optimized time-dependent detuning used to create the superposition. (b) Temporal evolution of the mode population of the two involved modes. (c) Temporal evolution of relative phase of the two quasi-modes at the center of their momentum distribution, see Fig. 5.

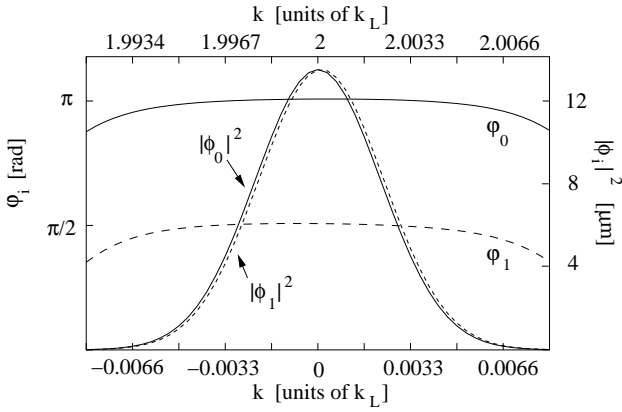


FIG. 5. Density profiles and phases of the two momentum modes after the optimization at $t = t_f$. The lower abscissa corresponds to the momentum wavefunction ϕ_0 with phase φ_0 centered around $k = 0$, the upper to ϕ_1 with phase φ_1 centered around $k = 2k_L$. Note that $p_1(t_f), p_2(t_f) \geq 0.475$.

V. SUMMARY AND CONCLUSION

In summary, we have demonstrated the usefulness of genetic algorithms in the control and manipulation of the quantum states of Bose-Einstein condensates. This was illustrated in two examples, the coherent population transfer between momentum states in a large condensate where the mean-field effects are important, and the creation of coherent superpositions of states of prescribed population and relative phase. We found that time-dependent Bragg scattering combined with the powerful optimization capabilities of genetic algorithms, provides a novel tool for quantum state design and coherent control in linear and nonlinear atom optics. The extension of these ideas to integrated atom optics appears particularly promising. Future theoretical work will generalize these concepts to systems with more degrees of freedom, such as e.g. multi-component condensates, and to additional control mechanisms such as time-dependent magnetic fields. The extension of this work to quantum-degenerate Bose-Fermi mixtures also appears promising.

ACKNOWLEDGMENTS

We thank J. V. Moloney for CPU time. This work is supported in part by the U.S. Office of Naval Research under Contract No. 14-91-J1205, by the National Science Foundation under Grant No. PHY98-01099, by the NASA Microgravity Program Grant NAG8-1775, by the U.S. Army Research Office, and by the Joint Services Optics Program.

APPENDIX A: DETAILS OF THE GENETIC ALGORITHM

In this Appendix we give specific details of the implementation of the genetic algorithm in the problem of BEC state engineering in an optical lattice.

Over the course of the optimization we monitor the maximum fitness f_{\max} of a population,

$$f_{\max} = \max\{f(c_i) : i = 1, \dots, \mathcal{N}\}. \quad (\text{A1})$$

Obviously, if at least the best chromosome is kept from the old generation, the maximum fitness is a monotonically increasing function. This feature, called “elitism”, is used throughout our simulations. Another observable of interest is the mean fitness f_{mean} of a population,

$$f_{\text{mean}} = \frac{1}{\mathcal{N}} \sum_{i=1}^{\mathcal{N}} f(c_i). \quad (\text{A2})$$

A typical evolution of these two quantities is shown in Fig. 6(a). The maximum fitness increases monotonically to reach a value close to the optimum after about 40 generations. In contrast, the mean fitness rises over the course of the first 10 generations and then exhibits fluctuations due to the stochastic character of the genetic algorithm: Parts of the population are replaced by randomly created chromosomes from one generation to the next and randomize the mean fitness value. In our simulations we used populations of size $\mathcal{N} = 50 - 100$ and performed the optimization over 50 – 100 generations. We always kept the best chromosomes of a generation and replaced 80% – 90% of the population by newly generated chromosomes. For the population transfer of Sec. IV A we used 16, and for the superposition state engineering of Sec. IV B 26 genes per chromosome. The gene boundaries were chosen as $-0.7\omega_R \leq a_{i\nu}, b_{i\nu} \leq 0.7\omega_R$.

As mentioned in Sec. III, we use an adaptive operator technique, where the operators themselves are dynamically assigned a fitness based on their performance. Choosing a particular mating operator via a roulette-wheel method [17] then assures that good operators are employed more often in the mating process. If any operator produces an offspring that is better than the best chromosome of the previous generation, we reward this operator by giving it a credit proportional to the increase in fitness it caused. Also, we pass half of this given credit back to the operator that created the parent chromosome involved in producing the better offspring. Thus operators that perform well and also their direct ancestors can accumulate credit over the run of the simulation. Passing credit back to previous operators enables us to reward pairs of operators that work well together at a certain stage of the optimization process. In our simulations we adjust the fitness of all operators every five generations based on the credit they accumulated during that period: The new operator fitness is then a weighted sum of the old fitness (the “basis portion”, in our case 85%) and

the accumulated credit (the “adaptive portion”, in our case 15%). The more credit an operator accumulates the higher will be its new fitness and the more likely it is that it will be chosen in future mating processes. Since the total operator fitness is set constant, we introduce a lower bound of 0.1 to the operator fitness, thereby preventing operators that do not perform well over several generations from being practically expelled from the pool of operators.

Fig. 6(b) shows a typical evolution of the fitness of the individual mating operators in the superposition state engineering problem from Sec. IV B. The creep and one-point-crossover operators perform well for the first 30 generations. For subsequent generations the two-point-crossover and the average-crossover operators take over and help increasing the maximum fitness, which approaches its optimum value (unity in the present example). There is no further improvement in the remaining 50 generations, the fitness of the various operators staying constant. The random mutation operators never perform well in the problem at hand. Consequently their fitness is quickly reduced to the lower bound. The creep operators, which are basically controlled mutations, perform much better and could replace the pure mutation operators.

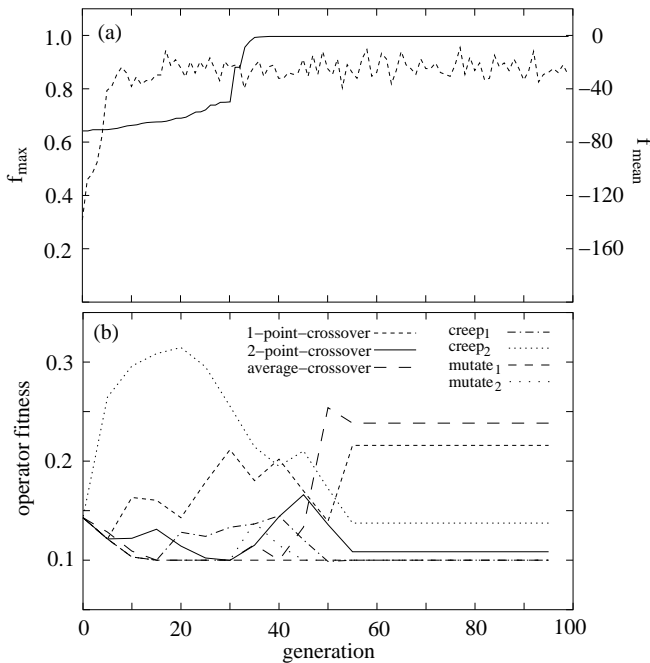


FIG. 6. A typical run of the genetic algorithm for the superposition state engineering: (a) Maximum fitness (solid) and mean fitness (dashed) of the population as a function of the generation. We started the optimization with pre-optimized chromosomes from previous simulations, which explains the high initial maximum fitness of over 60%. (b) Operator fitness as a function of the generation, starting with equal fitness for all operators. The minimum operator fitness is set equal to 0.1 for all operators.

- [1] S. Burger, K. Bongs, S. Dettmer, W. Ertmer, K. Sengstock, A. Sanpera, G. V. Shlyapnikov, and M. Lewenstein, Phys. Rev. Lett. **83**, 5198 (1999).
- [2] L. Dobrek, M. Gajda, M. Lewenstein, K. Sengstock, G. Birk, and W. Ertmer, Phys. Rev. A **60**, R3381 (1999).
- [3] J. Denschlag, J. E. Simsarian, D. L. Feder, C. W. Clark, L. A. Collins, J. Cubizolles, L. Deng, E. W. Hagley, K. Helmerson, W. P. Reinhardt, S. L. Rolston, B. I. Schneider, and W. D. Phillips, Science **287**, 97 (2000).
- [4] L. Deng, E. W. Hagley, J. Wen, M. Trippenbach, Y. Band, P. S. Julienne, J. E. Simsarian, K. Helmerson, S. L. Rolston, and W. D. Phillips, Nature **398**, 218 (1999).
- [5] S. Inouye, T. Pfau, S. Gupta, A. P. Chikkatur, A. Gorlitz, D. E. Pritchard, and W. Ketterle, Nature **402**, 641 (1999).
- [6] S. Inouye, A. P. Chikkatur, D. M. Stamper-Kurn, J. Stenger, D. E. Pritchard, and W. Ketterle, Science **285**, 571 (1999).
- [7] C. K. Law and N. P. Bigelow, Phys. Rev. A **58**, 4791 (1998).
- [8] M. G. Moore and P. Meystre, Phys. Rev. Lett. **83**, 5202 (1999).
- [9] P. Meystre, *Atom Optics*, Springer Verlag, New York (2001), in press.
- [10] B. P. Anderson and M. A. Kasevich, Science **282**, 1686 (1998).
- [11] U. Drodofsky, J. Stuhler, B. Brezger, T. Schulze, M. Drewsen, T. Pfau, and J. Mlynek, Microelectronic Engineering **35**, 285 (1997).
- [12] K. S. Johnson, J. H. Thywissen, N. H. Dekker, K. K. Berggren, A. P. Chu, R. Younkin, and M. Prentiss, Science **280**, 1583 (1998).
- [13] O. Zobay, E. V. Goldstein, and P. Meystre, Phys. Rev. A **60**, 3999 (1999).
- [14] T. C. Weinacht, J. Ahn, P. H. Bucksbaum, Nature **397**, 233 (1999).
- [15] M. Olshanii, N. Dekker, C. Herzog, and M. Prentiss, Phys. Rev. A **62**, 033612 (2000).
- [16] R. S. Judson and H. Rabitz, Phys. Rev. Lett. **68**, 1500 (1992).
- [17] L. Ed. Davis, *Handbook of Genetic Algorithms* (Van Norstrand Reinhold, New York, 1991).
- [18] D. A. Coley, *An Introduction to Genetic Algorithms for Optimization* (Addison Wesley, Reading, MA, 1999).

Scientists and Engineers (World Scientific, Singapore, 1999).

- [19] R. Carretero-González and K. Promislow, cond-mat/0105600 (2001).
- [20] V. Milner, J. L. Hanssen, W. C. Campbell, and M. G. Raizen, Phys. Rev. Lett. **86**, 1514 (2001).
- [21] J. Stenger, S. Inouye, A. P. Chikkatur, D. M. Stamper-Kurn, D. E. Pritchard, and W. Ketterle, Phys. Rev. Lett. **82**, 4569 (1999).
- [22] E. W. Hagley, L. Deng, M. Kozuma, M. Trippenbach, Y. B. Band, M. Edwards, M. Doery, P. S. Julienne, K. Helmerson, S. L. Rolston, and W. D. Phillips, Phys. Rev. Lett. **83**, 3112 (1999).
- [23] J. E. Simsarian, J. Denschlag, M. Edwards, C. W. Clark, L. Deng, E. W. Hagley, K. Helmerson, S. L. Rolston, and W. D. Phillips, Phys. Rev. Lett. **85**, 2040 (2000).
- [24] M. Kozuma, L. Deng, E. W. Hagley, J. Wen, R. Lutwak, K. Helmerson, S. L. Rolston, and W. D. Phillips, Phys. Rev. Lett. **82**, 871 (1999).
- [25] Q. Niu, X.-G. Zhao, G. A. Georgakis, and M. G. Raizen, Phys. Rev. Lett. **76**, 4504 (1996).
- [26] C. F. Bharucha, K. W. Madison, P. R. Morrow, S. R. Wilkinson, B. Sundaram, and M. G. Raizen, Phys. Rev. A **55**, R857 (1997).
- [27] M. B. Dahan, E. Peik, J. Reichel, Y. Castin, and C. Salomon, Phys. Rev. Lett. **76**, 4508 (1996).
- [28] E. Peik, M. Ben Dahan, I. Bouchoule, Y. Castin, and C. Salomon, Appl. Phys. B **65**, 685 (1997).
- [29] E. Peik, M. B. Dahan, I. Bouchoule, Y. Castin, and C. Salomon, Phys. Rev. A **55**, 2989 (1997).
- [30] O. Morsch, J. H. Müller, M. Cristiani, and E. Arimondo, cond-mat/0103466 (2001).
- [31] F. S. Cataliotti, S. Burger, C. Fort, P. Maddaloni, F. Minardi, A. Trombettoni, A. Smerzi, and M. Inguscio, Science **293**, 843 (2001).
- [32] C. Cohen-Tannoudji, in *Fundamental Systems in Quantum Optics*, edited by J. Dalibard, J.-M. Raimond, and J. Zinn-Justin (North-Holland, Amsterdam, 1992).
- [33] S. Pötting, M. Cramer, C. H. Schwalb, H. Pu, and P. Meystre, Phys. Rev. A **64**, 023604 (2001).
- [34] D. Jaksch, C. Bruder, J. I. Cirac, C. W. Gardiner, and P. Zoller, Phys. Rev. Lett. **81**, 3108 (1998).
- [35] C. Raman, M. Köhl, R. Onofrio, D. S. Durfee, C. E. Kuklewicz, Z. Hadzibabic, and W. Ketterle, Phys. Rev. Lett. **83**, 2502 (1999).
- [36] R. Onofrio, C. Raman, J. M. Vogels, J. R. Abo-Shaeer, A. P. Chikkatur, and W. Ketterle, Phys. Rev. Lett. **85**, 2228 (2000).
- [37] S. Burger, F. S. Cataliotti, C. Fort, F. Minardi, M. Inguscio, M. L. Chiofalo, and M. P. Tosi, Phys. Rev. Lett. **86**, 4447 (2001).
- [38] B. J. Pearson, J. L. White, T. C. Weinacht, and P. H. Bucksbaum, Phys. Rev. A **63**, 063412 (2001).
- [39] D. Choi and Q. Niu, Phys. Rev. Lett. **82**, 2022 (1999).
- [40] P. B. Blakie and R. J. Ballagh, J. Phys. B: At. Mol. Opt. Phys. **33**, 3961 (2000).
- [41] The relatively fast initial increase of the detuning above the level of the first Bragg resonance makes up for the fact that at $t = 0$ we start with zero detuning and couple to negative momentum modes.